SEARCHES FOR GRAVITATIONAL WAVES FROM NEARBY SUPERNOVAE

Ornella Juliana Piccinni for the LIGO-Virgo-KAGRA collaboration,
L'Oreal-UNESCO fellow
INFN, Rome 1

INFN Istituto Nazionale di Fisica Nucleare
LIGO VIRGO
For Women in Science
FONDATION L'OREAL

TeVPA 2021, 25-29 Oct 2021

OVERVIEW

- Continuous gravitational waves (CW) signals and sources
- Main emission models
- Are supernova remnant good targets?
- Latest search for CW from supernova remnants
  - sources
  - methods
  - results and implications
- Prospects for O4
- Final remarks

GRAVITATIONAL WAVE SOURCES

	Modeled waveform	*Unmodeled waveform*
Long-lived *$T \sim$ months or years*	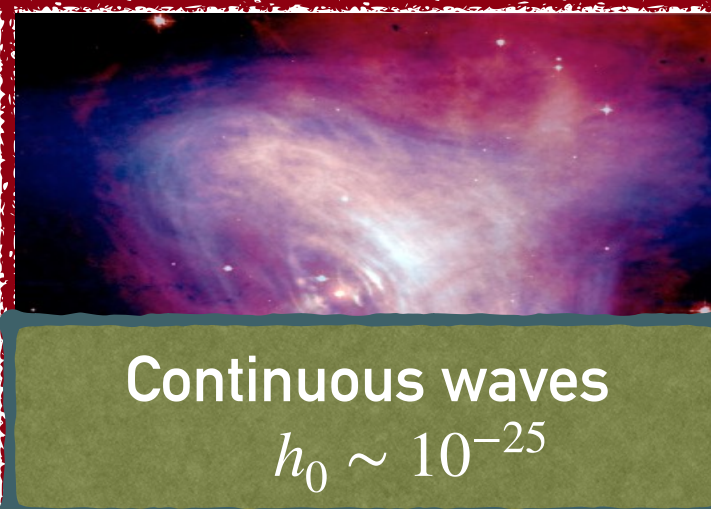 **Continuous waves** $h_0 \sim 10^{-25}$	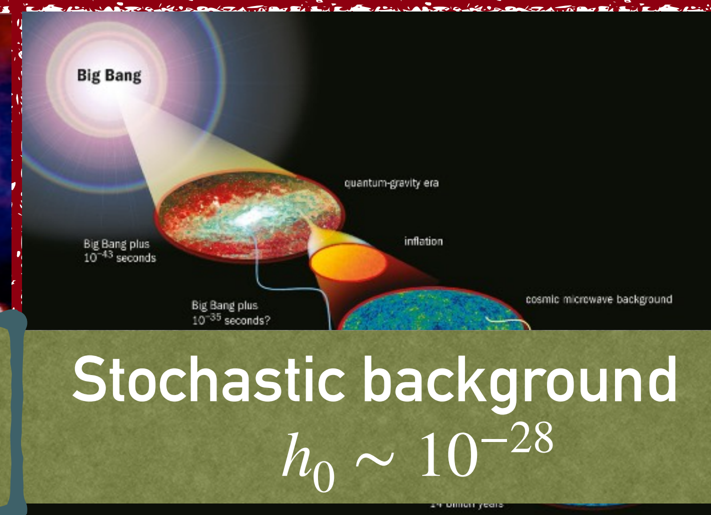 **Stochastic background** $h_0 \sim 10^{-28}$
Transients *$T \sim$ up to minutes*	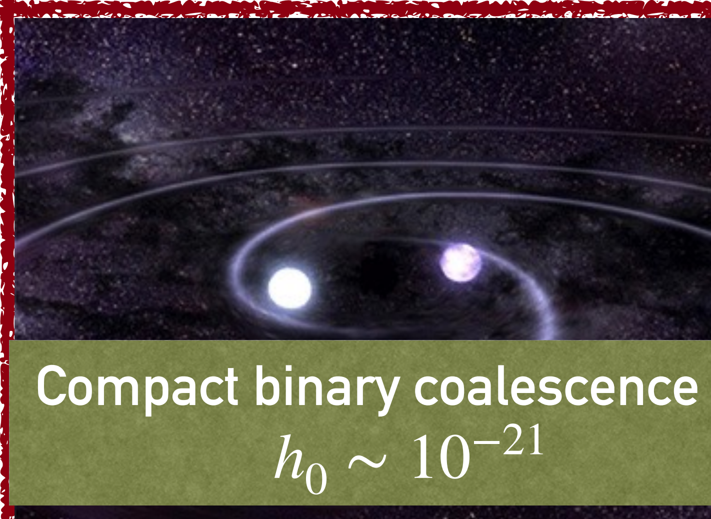 **Compact binary coalescence** $h_0 \sim 10^{-21}$	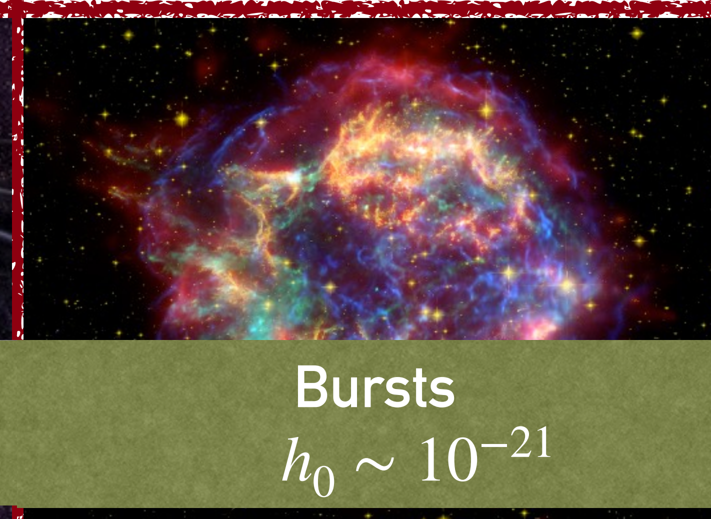 **Bursts** $h_0 \sim 10^{-21}$

WHAT IS A CONTINUOUS WAVE (CW)?

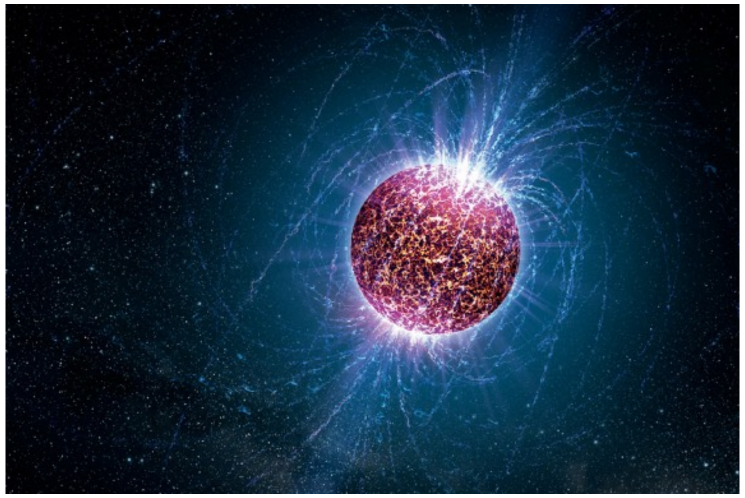

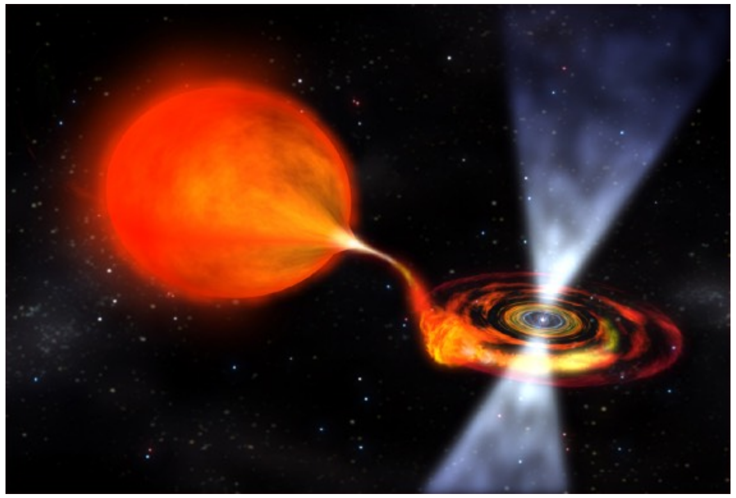

Credit: C. Reed, Penn State/Mc Gill University

Persistent signal (long-lived)

Produced by a nearly **periodic** mass quadrupole moment variation

Expected sources

Non-axisymmetric isolated neutron stars (NS)

NSs in binary systems (e.g. in accreting systems)

More objects: bosons clouds around spinning BH, newborn NSs

Expected strain

$$h_0 \cong 10^{-27} \left(\frac{I_3}{10^{38}\ \mathrm{kg\ m^2}}\right) \left(\frac{10\,\mathrm{kpc}}{d}\right) \left(\frac{f}{100\ \mathrm{Hz}}\right)^2 \left(\frac{\epsilon}{10^{-6}}\right) \ll h_{0_{CBC}}$$

[For a CW review: Lasky PASA 32, pp. 34 (2015), Riles Mod Phys Lett A 32, No. 39, 1730035 (2017)]

MAIN EMISSION MODELS

Triaxial rotor spinning about one of the principle axes (no precession) $f = 2f_\star$ (theta=0)

Pinned superfluid to the crust (pinning not aligned with principal axes) $f_1 = 2f_\star$ and $f_2 = f_\star$ (no precession, grey region)

Jones 2010; Bejger & Krolak 2014;

r-mode emission $f = 4f_\star/3$

Lasky PASA 32, pp. 34 (2015)

precession and more: emission occurs at multiple harmonics

Zimmermann M and Szedenits E Jr 1979 Phys. Rev. D 20 351, Van Den Broeck 2005;

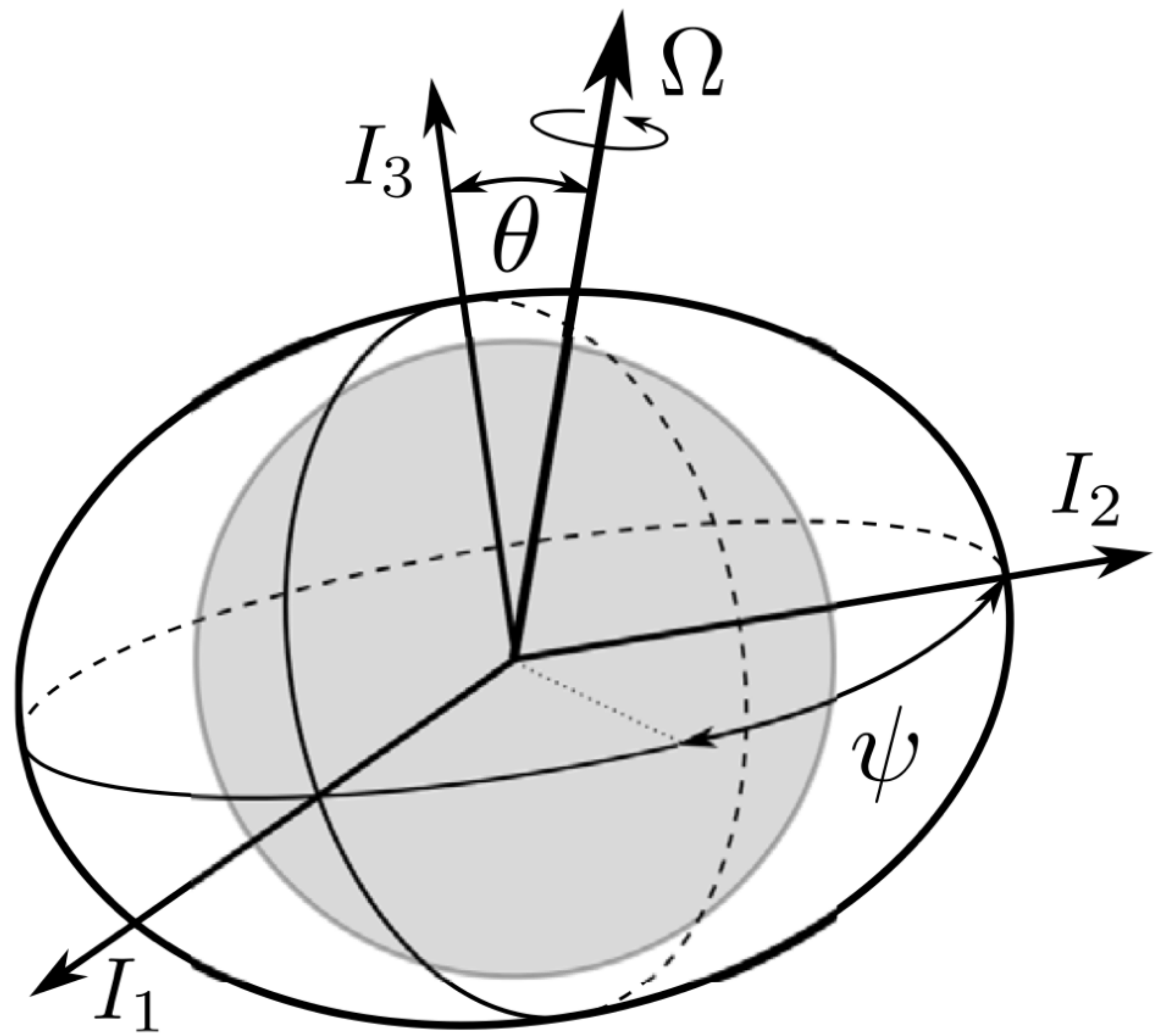

M. Bejger and A. Królak 2014 Class. Quantum Grav. 31 105011

EASY CASE: ISOLATED NEUTRON STAR

$$h_0 \cong 10^{-27} \left(\frac{I_3}{10^{38}\ \mathrm{kg\,m^2}}\right)\left(\frac{10\,\mathrm{kpc}}{d}\right)\left(\frac{f}{100\ \mathrm{Hz}}\right)^2\left(\frac{\epsilon}{10^{-6}}\right) \ll h_{0_{CBC}}$$

non-precessing, rotating around one of the axes

here $f = 2f_\star$

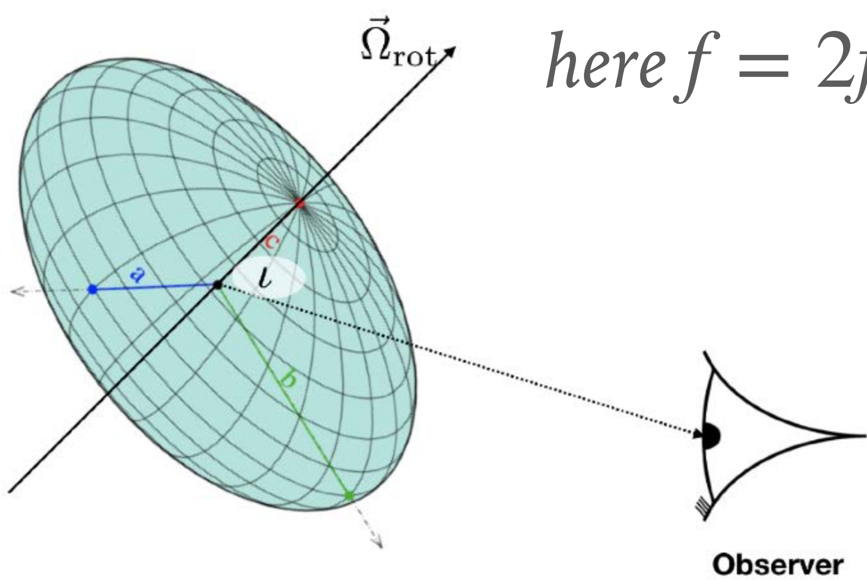

Tri-axial spinning neutron star

Credit: S. Mastrogiovanni

$$h_0 = \frac{4\pi^2 G}{c^4}\frac{I_3 f^2}{d}\epsilon$$

I_3: moment of inertia

ϵ: ellipticity

$$\epsilon = \left|\frac{I_1 - I_2}{I_3}\right|$$

What is the actual value of ϵ*?*

$$\epsilon < 2\times 10^{-5}\left(\frac{u_{break}}{0.1}\right) \textit{ crustal strain} \qquad \epsilon \approx 10^{-12}\left(\frac{B}{10^{12}\mathrm{G}}\right)^2 \textit{ magnetic field}$$

N. Andersson et al. 2009

ESTIMATES ON THE ELLIPTICITY

Theoretical models K. Glampedakis & L. Gualtieri [Astro. and Space Science Lib., vol 457. Springer, 2018]

- Solid strange quark stars: $\epsilon \leq 6 \times 10^{-4}$
- Hybrid and meson condensates stars: $\epsilon \leq 3 - 9 \times 10^{-6}$
- Canonical magnetic deformations: $\epsilon \leq 2 - 7 \times 10^{-7}$
- Buried magnetic field in MSPs: $\epsilon_{fid} \sim 10^{-9}$ and a buried magnetic field of 10^{11} G. Woan+[ApJL,863:L40, 2018]

Above models more stringent than older results Johnson-McDaniel+ [PRD 88, 044004 (2013)]

- normal NS matter: $\epsilon \leq 10^{-5}$
- hybrid stars: $\epsilon \leq 10^{-3}$
- extreme quark stars: $\epsilon \leq 10^{-1}$

Larger mountains might be provided by nature, depending upon the high density equation of state.

THE SIGNAL AT THE DETECTOR

Credit: K. Wette

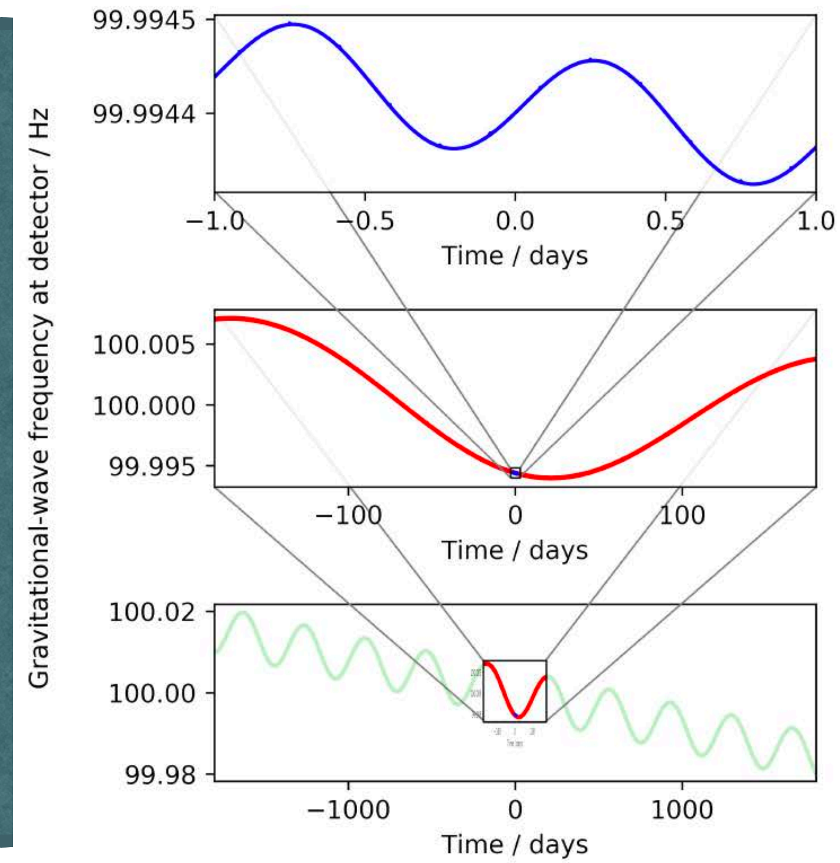

A CW received at the detector is NOT exactly monochromatic

- SPIN-DOWN due to the loss of energy of the star

  $\dot{f} \propto f^n$ EM (n~3), GW (n=5), r-mode (n=7)

- DOPPLER shift due to the motion of the Earth

  $$f(t) = f_0 \left(1 + \frac{\vec{v} \cdot \hat{n}}{c}\right)$$ daily+yearly cycle

- SIDEREAL VARIATION of the amplitude

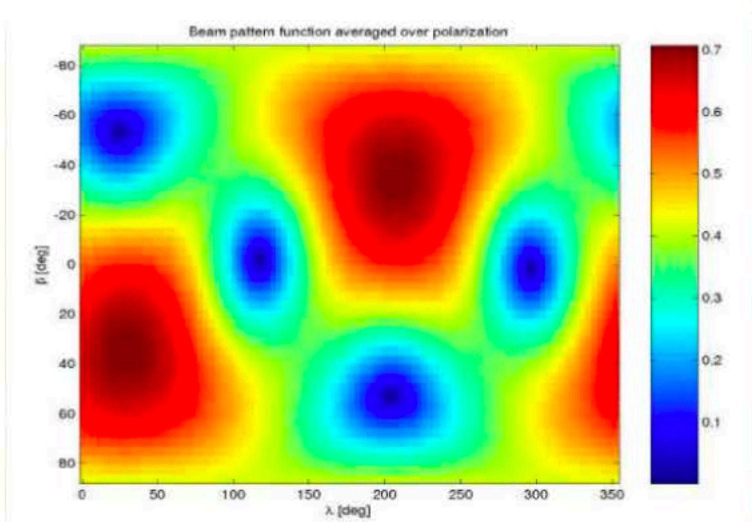

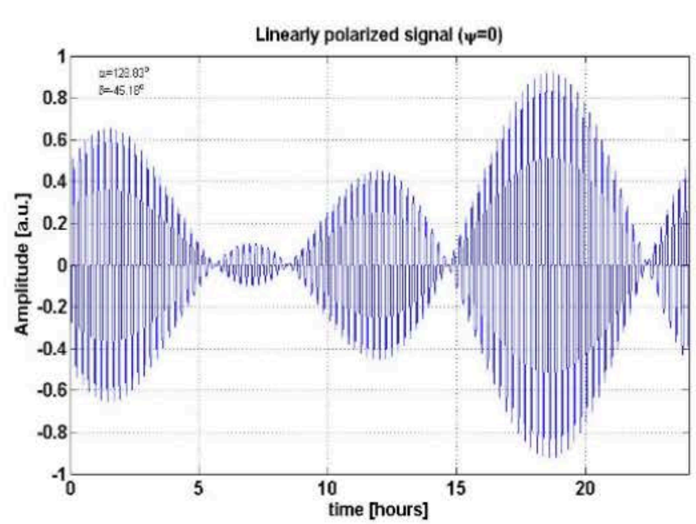

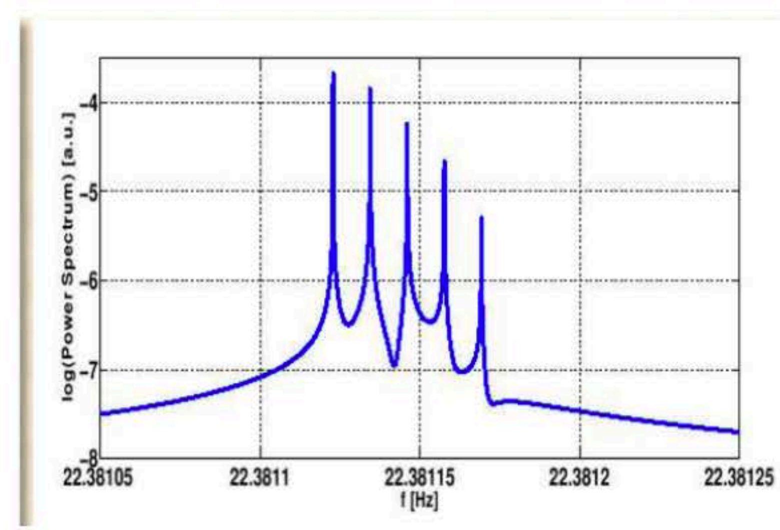

TYPE OF CW SEARCHES FOR ISOLATED NS

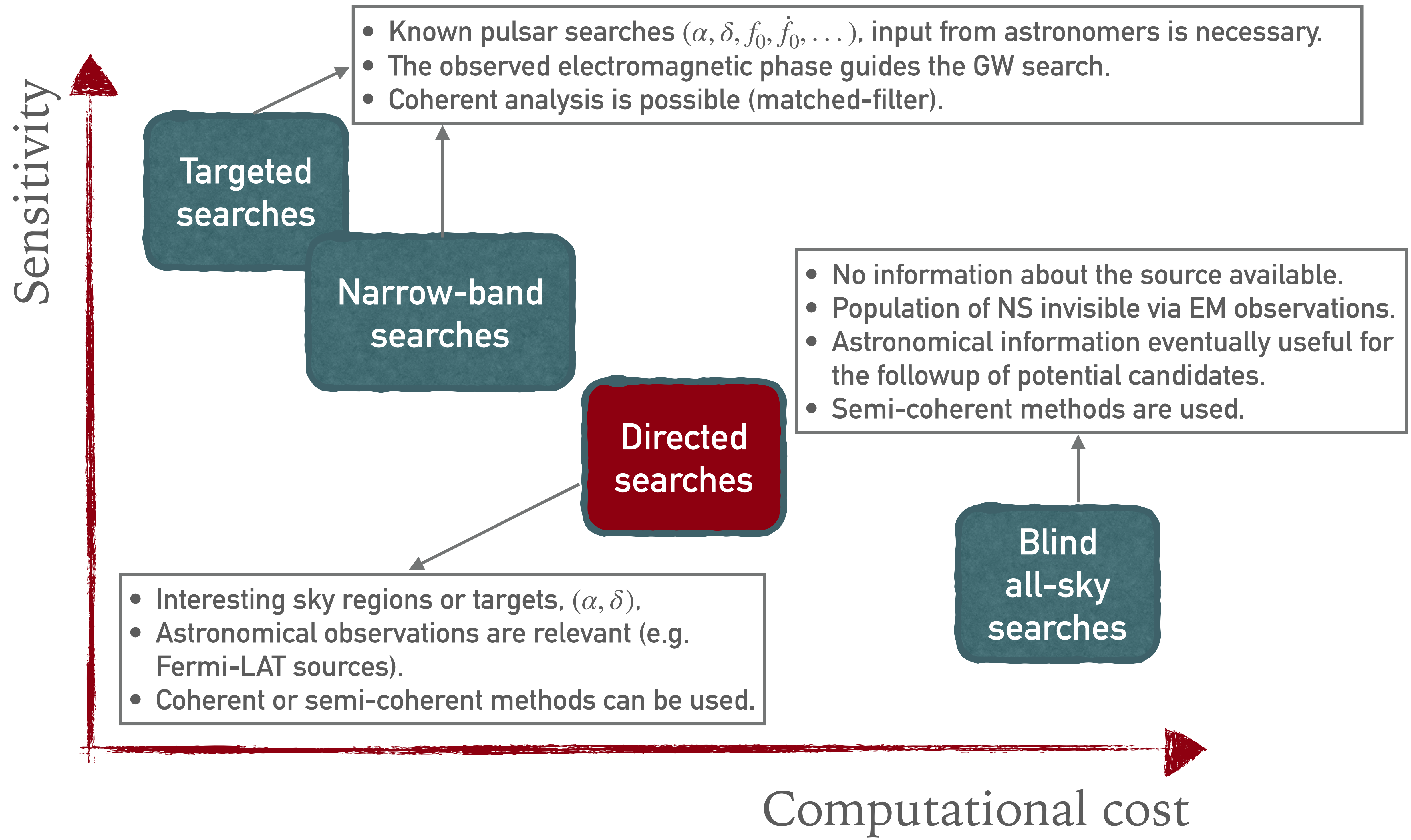

HOW LIKELY IS A DETECTION OF A SPINNING DEFORMED STAR?

- All the rotational energy becomes gravitational radiation
- For known pulsars this is the spin-down limit
- Age-based upper limits h_0^{age} on the gravitational wave strain *guessing* the age and distance of the source (Wette 2008)

$$h_0^{\mathrm{age}} = 2.2 \times 10^{-24} \left(\frac{1\mathrm{kpc}}{d}\right)\left(\frac{1\mathrm{kyr}}{t_{\mathrm{age}}}\right)^{1/2} \left(\frac{I_3}{10^{38}\ \mathrm{kg\ m}^2}\right)^{1/2}$$

- $h_0^{\mathrm{age}} >$ search sensitivity, promising target
- These quantities can be translated in terms of the star ellipticity and ϵ^{age}

ARE YOUNG SNR GOOD TARGETS?

LVK, arXiv:2105.11641

Searches for continuous gravitational waves from young supernova remnants in the early third observing run of Advanced LIGO and Virgo

- Many young supernova remnants (SNRs) contain central compact objects, which are likely to be young neutron stars
- Age estimates define the frequency/spin-down range to search
- Distance estimates define the maximum expected signal strength h_0^{age} and guide where to search
- Young neutron stars are likely to be non-axisymmetric
- Young neutron stars rotate more rapidly
- Tracking large spin-down ($\dot{f}$) is expensive
- We need efficient algorithms to search a large number of targets

DATA

LVK, arXiv:2105.11641

- Latest data from LIGO and Virgo - first half of O3
- Six months from April to October 2019 (O3a)
- Three complementary pipelines:
  - Band-Sampled Data (BSD)
  - the single-harmonic Viterbi (SHV)
  - the dual-harmonic Viterbi (DHV)
- Up to 15 targets investigated, up to 2kHz

THREE PIPELINES ONE SEARCH: SUPERNOVA REMNANTS O3A

Source	Age (kyr)	Distance (kpc)	Right ascension (h:m:s)	Declination (°:′:″)	References
G18.9–1.1	2.6–6.1	1.6–2.5	18:29:13.1	−12:51:13	Ranasinghe et al. (2019); Shan et al. (2018) Harrus et al. (2004)
G39.2–0.3/3C 396	3–7.3	6.2–8.5	19:04:04.7	5:27:12	Shan et al. (2018); Su et al. (2010) Harrus & Slane (1999)
G65.7+1.2/DA 495	7–20	1–5	19:52:17.0	29:25:53	Karpova et al. (2015); Kothes et al. (2008)
G93.3+6.9/DA 530	2.9–7	1.7–3.5	20:52:14.0	55:17:22	Straal & van Leeuwen (2019); Jiang et al. (2007) Landecker et al. (1999); Foster & Routledge (2003)
G189.1+3.0/IC 443	3–30	1.4–1.9	06:17:05.3	22:21:27	Ambrocio-Cruz et al. (2017); Kargaltsev et al. (2017) Swartz et al. (2015); Fesen & Kirshner (1980)
G266.2–1.2/Vela Jr.	0.69–5.1	0.2–1	08:52:01.4	−46:17:53	Allen et al. (2014); Liseau et al. (1992)
G353.6–0.7	10–40	3.2–6.1	17:32:03.3	−34:45:18	Klochkov et al. (2015); Fukuda et al. (2014) Tian et al. (2008)
G1.9+0.3	0.10–0.26	8.5–10	17:48:46.9	−27:10:16	Reynolds et al. (2008); Roy & Pal (2014)
G15.9+0.2	0.54–5.7	6.0–16.7	18:18:52.1	−15:02:14	Reynolds et al. (2006); Sasaki et al. (2018)
G111.7–2.1/Cas A	0.28–0.35	3.3–3.4	23:23:27.9	58:48:42	Ilovaisky & Lequeux (1972); Reed et al. (1995); van den Bergh (1971); Fesen et al. (2006)
G291.0–0.1/MSH 11–62	1.2–10	3.0–10	11:11:48.6	−60:39:26	Roger et al. (1986); Moffett et al. (2001); Harrus et al. (2004); Slane et al. (2012)
G330.2+1.0	0.8–9.8	4.9–10	16:01:03.1	−51:33:54	McClure-Griffiths et al. (2001); Park et al. (2009); Borkowski et al. (2018); Leahy et al. (2020)
G347.3–0.5	0.1–6.8	0.9–6.0	17:13:28.3	−39:49:53	Slane et al. (1999); Wang et al. (1997); Cassam-Chenai et al. (2004); Lazendic et al. (2003) Tsuji & Uchiyama (2016)
G350.1–0.3	0.6–2.5	4.5–9.0	17:20:54.5	−37:26:52	Gaensler et al. (2008); Lovchinsky et al. (2011) Yasumi et al. (2014); Leahy et al. (2020)
G354.4+0.0	0.1–0.5	5–8	17:31:27.5	−33:34:12	Roy & Pal (2013)

BSD,DHV (first seven sources)

Green SNR & Manitoba SNRcat (last eight sources)

SHV (all sources)

BAND SAMPLED DATA PIPELINE– SNR O3A

Source	minimum t_{age} (kyr)	T_{coh} (hr) (@100 Hz)	f (Hz)	$\dot{f}$ (Hz s^{-1}) (@100 Hz)
G65.7+1.2, G189.1+3.0, G266.2–1.2	3	8	[10, 600]	$[-1.06 \times 10^{-9}, 1.06 \times 10^{-10}]$
G353.6–0.7	27	8	[10, 1000]	$[-1.17 \times 10^{-10}, 1.17 \times 10^{-11}]$
G18.9–1.1	4.4	8	[10, 1000]	$[-7.13 \times 10^{-10}, 7.13 \times 10^{-11}]$
G39.2–0.3	4.7	8	[10, 1000]	$[-6.75 \times 10^{-10}, 6.75 \times 10^{-11}]$
G93.3+6.9	5	8	[10, 1000]	$[-6.34 \times 10^{-10}, 6.34 \times 10^{-11}]$

- Method based on the FrequencyHough
- Triaxial rotor model
- 2.5 hr $\leq T_{coh} \leq$ 17.8 hr
- first stage candidates: 42464
- follow-up analyses on 35
- no surviving candidates left

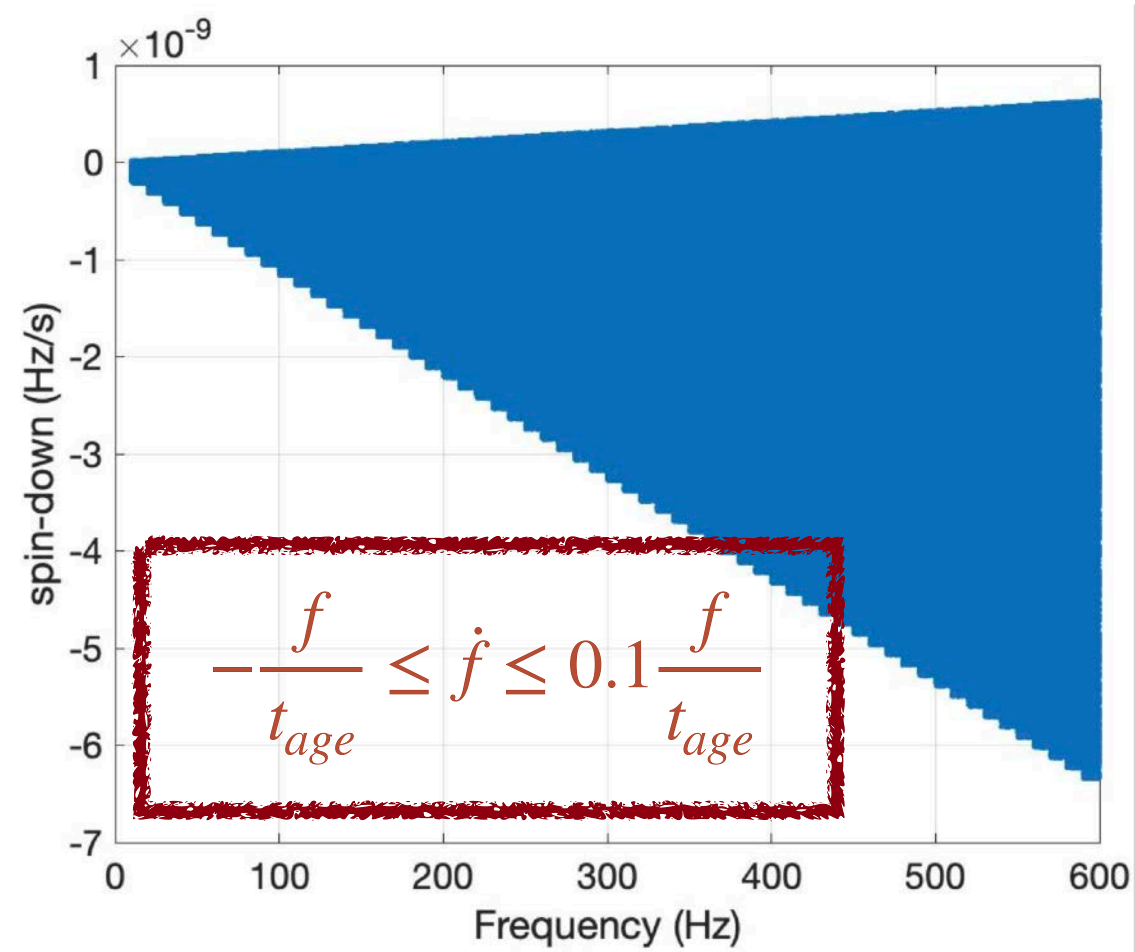

G65.7+1.2

Piccinni et al. (2020)

SINGLE HARMONIC VITERBI – SNR O3A

Source	Minimum $t_{\rm age}$ (kyr)	D (kpc)	$T_{\rm coh}$ (hours)	f (Hz)	$\dot{f}$ (Hz/s)
G1.9+0.3	0.10	8.5	1.0	$[31.56, 121.7]$	$[-3.858\times10^{-8}, 3.858\times10^{-8}]$
G15.9+0.2	0.54	8.5	1.0	$[44.03, 657.1]$	$[-3.858\times10^{-8}, 3.858\times10^{-8}]$
G18.9–1.1	4.4	2	1.9	$[31.02, 1511]$	$[-1.507\times10^{-8}, 1.507\times10^{-8}]$
G39.2–0.3	3.0	6.2	2.8	$[62.02, 459.2]$	$[-1.968\times10^{-8}, 1.968\times10^{-8}]$
G65.7+1.2	20	1.5	4.7	$[35.10, 1128]$	$[-3.149\times10^{-9}, 3.149\times10^{-9}]$
G93.3+6.9	5.0	1.7	1.9	$[30.00, 1668]$	$[-1.335\times10^{-8}, 1.335\times10^{-8}]$
G111.7–2.1	0.30	3.3	1.0	$[25.71, 365.1]$	$[-3.858\times10^{-8}, 3.858\times10^{-8}]$
G189.1+3.0	3.0	1.5	1.4	$[26.13, 2000]$	$[-1.968\times10^{-8}, 1.968\times10^{-8}]$
G266.2–1.2	0.69	0.2	1.0	$[18.36, 839.6]$	$[-3.858\times10^{-8}, 3.858\times10^{-8}]$
G291.0–0.1	1.2	3.5	1.0	$[31.97, 1460]$	$[-3.858\times10^{-8}, 3.858\times10^{-8}]$
G330.2+1.0	1.0	5	1.1	$[36.57, 1039]$	$[-3.858\times10^{-8}, 3.858\times10^{-8}]$
G347.3–0.5	1.6	0.9	1.0	$[21.74, 1947]$	$[-3.858\times10^{-8}, 3.858\times10^{-8}]$
G350.1–0.3	0.60	4.5	1.0	$[31.96, 730.1]$	$[-3.858\times10^{-8}, 3.858\times10^{-8}]$
G353.6–0.7	27	3.2	10	$[77.86, 318.3]$	$[-2.295\times10^{-9}, 2.295\times10^{-9}]$
G354.4+0.0	0.10	5	1.0	$[25.72, 121.7]$	$[-3.858\times10^{-8}, 3.858\times10^{-8}]$

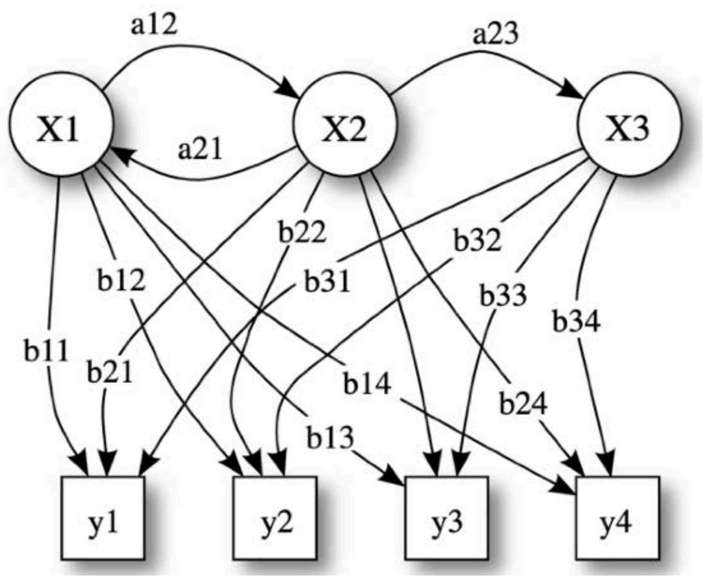

$$a_{X_iX_i} = a_{X_{i\pm1}X_i} = 1/3$$

$$T_{\rm coh} \propto \left|\dot{f}^{\rm max}\right|^{-1/2}$$

- Viterbi use Hidden Marcov Model tracking
- Single harmonic model
- 15 targets, larger spin down range
- first stage candidates: 42464
- follow-up analyses on 1
- no surviving candidates left

Sun et al. (2018)

DUAL HARMONIC VITERBI – SNR O3A

Source	Minimum $t_{\rm age}$ (kyr)	$T_{\rm coh}$ (hr)	$f_\star$ (Hz)	$\dot{f}_\star$ (Hz s^{-1})
G65.7+1.2	20	12	[50, 338]	$[-1.34 \times 10^{-10}, 0]$
G189.1+3.0	20	12	[50, 338]	$[-1.34 \times 10^{-10}, 0]$
G353.6–0.7	27	12	[50, 457]	$[-1.34 \times 10^{-10}, 0]$
G18.9–1.1	4.4	9	[50, 132]	$[-2.38 \times 10^{-10}, 0]$
G39.2–0.3	3	9	[50, 90]	$[-2.38 \times 10^{-10}, 0]$
G93.3+6.9	5	9	[50, 150]	$[-2.38 \times 10^{-10}, 0]$
G266.2–1.2	5.1	9	[50, 153]	$[-2.38 \times 10^{-10}, 0]$

$$\left|\dot{f}_\star\right| \in \left[0, 1/\left(4T_{\rm coh}^2\right)\right]$$

- HMM scheme tracking simultaneously 2 frequencies
- signal frequency evolution dominated by secular spin down, negatively biased random walk $a_{X_{i-1}X_i} = a_{X_iX_i} = 1/2$.
- first stage candidates: 477
- followup 25
- no surviving candidates left

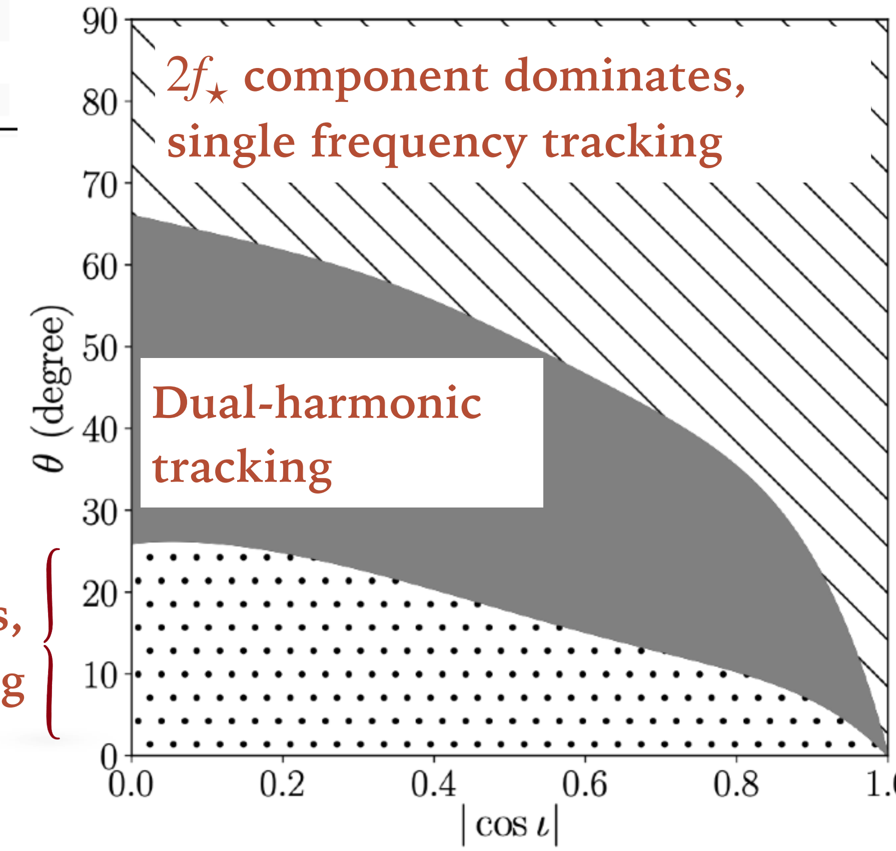

L. Sun, A.Melatos, and P. D. Lasky
Phys. Rev. D **99**, 123010 (2019)

RESULTS – SNR O3A

LVK, arXiv:2105.11641

- For the triaxial rotator model best result 7.7×10^{-26} (G39.2-0.3) for the BSD, similar for other targets
- For the random-walk signal model (SHV), larger range of spin-down and stochastic spin wandering
- For DHV model linear polarization for both $f_\star$ and $2f_\star$ is assumed
- DHV cannot set a confidence limit without an explicit assumption of the inclination and wobble angles

$\theta = \pi/4 \quad \cos\iota = 1$

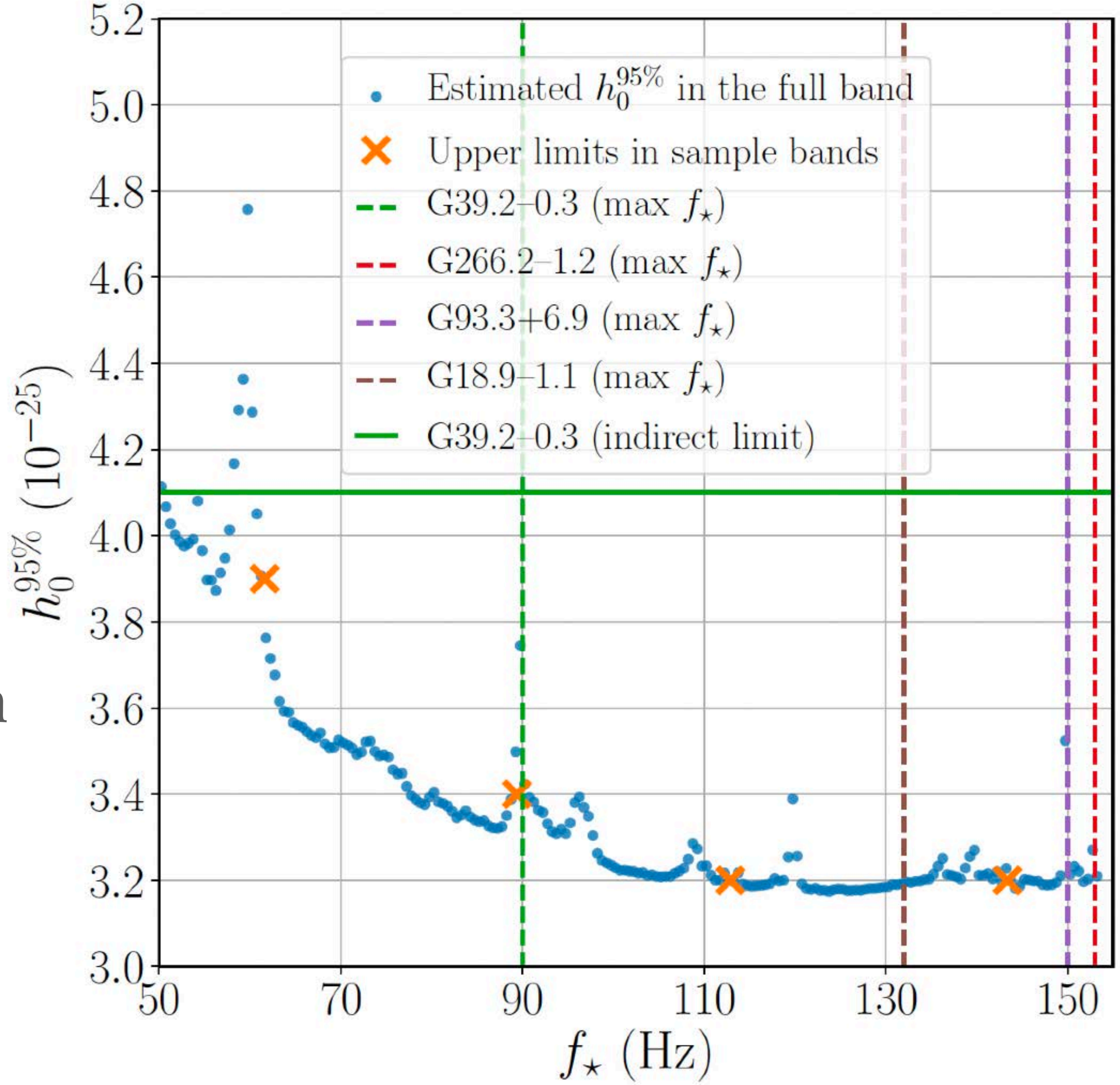

(b) G18.9–1.1, G39.2–0.3, G93.3+6.9, G266.2–1.2

ELLIPTICITY AND R-MODE - SNR O3A

LVK, arXiv:2105.11641

$$\epsilon = 9.5 \times 10^{-5} \left(\frac{h_0}{10^{-24}}\right) \left(\frac{d}{1\text{kpc}}\right) \left(\frac{100\ \text{Hz}}{f}\right)^2$$

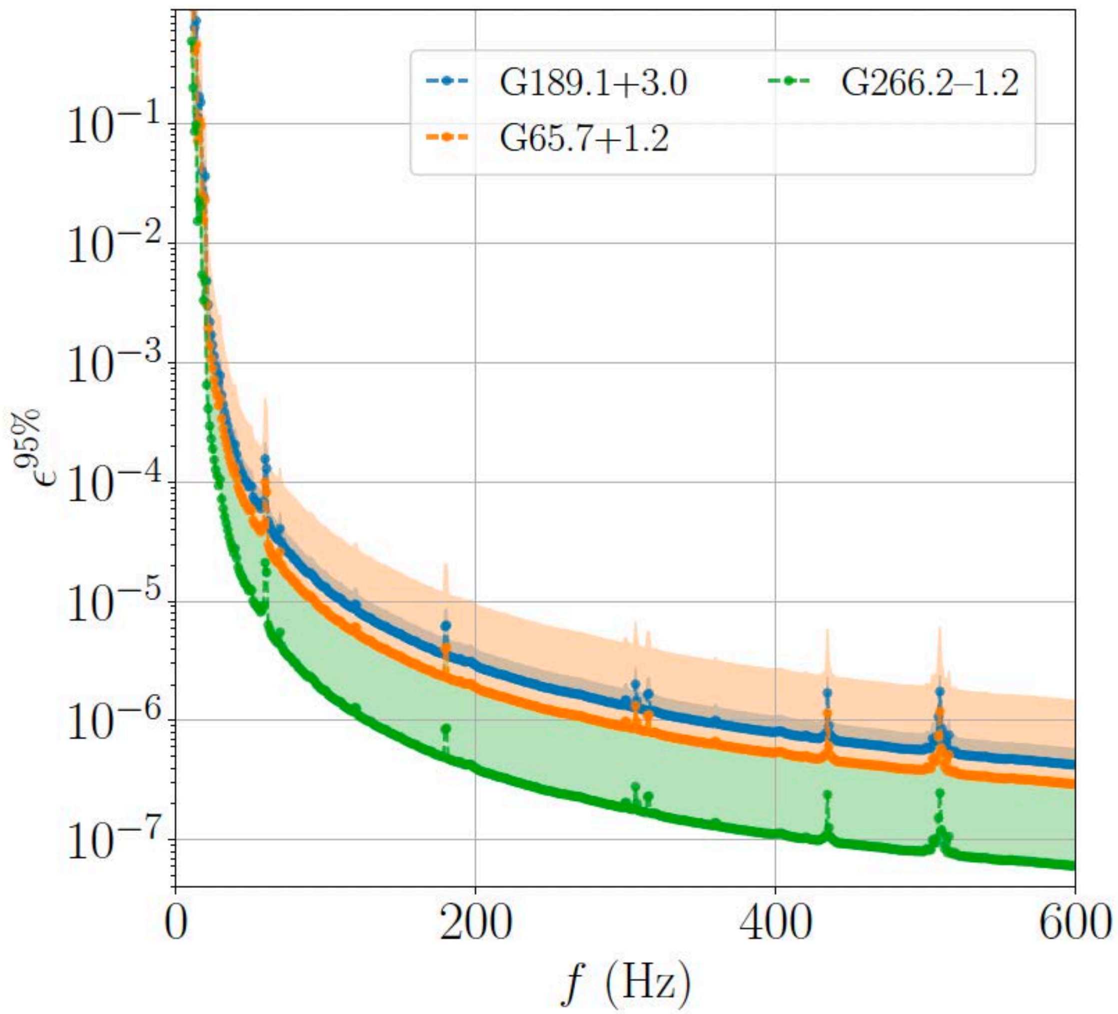

$$\alpha \simeq 0.028 \left(\frac{h_0}{10^{-24}}\right) \left(\frac{d}{1\text{kpc}}\right) \left(\frac{100\ \text{Hz}}{f}\right)^3$$

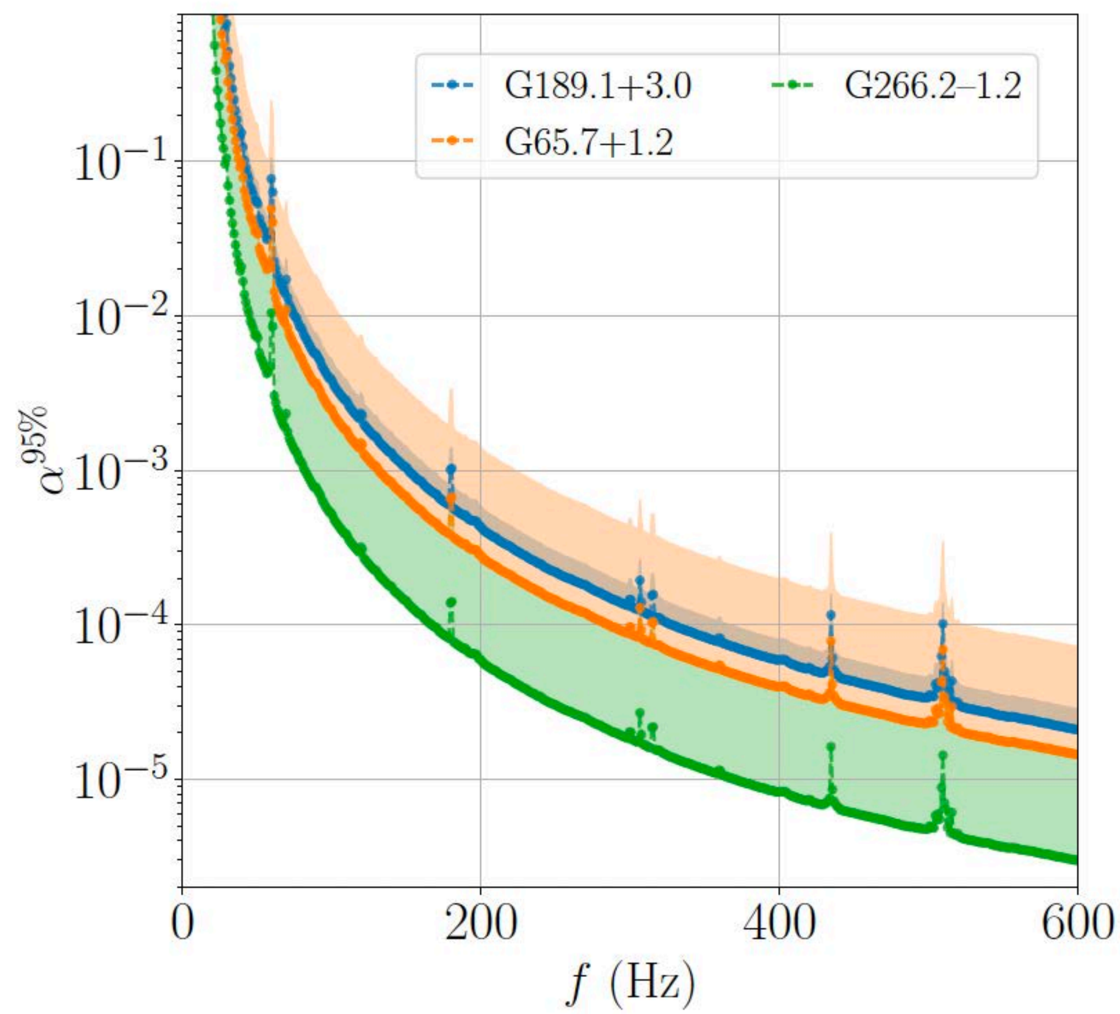

- Ellipticity $\epsilon < 10^{-6}$ for most of the sources; less than theoretical limit for normal neutron stars (Johnson-McDaniel & Owen 2013), 6×10^{-8} for the closest source Vela Jr
- r-mode amplitude $\alpha < 10^{-3}$, reaching below the theoretical prediction expected for the nonlinear saturation mechanisms (Bondarescu et al. 2009)
- The signal model adopted by DHV search cannot be interpreted as current quadrupole emission from an r-mode

COMPARISON TO LITERATURE

- Results from BSD are:
  - 2.5x more stringent than Abbott et al. (2019)
  - 1.3x more stringent than Lindblom & Owen (2020)
- Abbott et al (2019): $h_0^{95\%} = 2 \times 10^{-25}$ for most sources, $h_0^{95\%} = 1 \times 10^{-25}$ for one source in O1 data.
- Lindblom & Owen (2020) same method of Abbott et al. (2019) in O2 data: $h_0^{95\%} = 1 \times 10^{-25}$ for G65.7+1.2

- Our results with BSD for Vela Jr improve on the Papa et al. (2020)
- Our SHV $h_0^{95\%}$ for Cas A and G347.3-0.5 are beaten by Papa et al. (2020) but use a signal model with stochastic spin wandering
- Papa et al. (2020) present a deep search in O2 data:
  - $h_0^{90\%} = 1.2 \times 10^{-25}$, Cas A
  - $h_0^{90\%} = 9.3 \times 10^{-26}$, Vela Jr
  - $h_0^{90\%} = 8.8 \times 10^{-26}$, G347.3-0.5

WHAT'S NEXT?

FUTURE PROSPECTS: VELA JR. SEARCH ELLIPTICITY

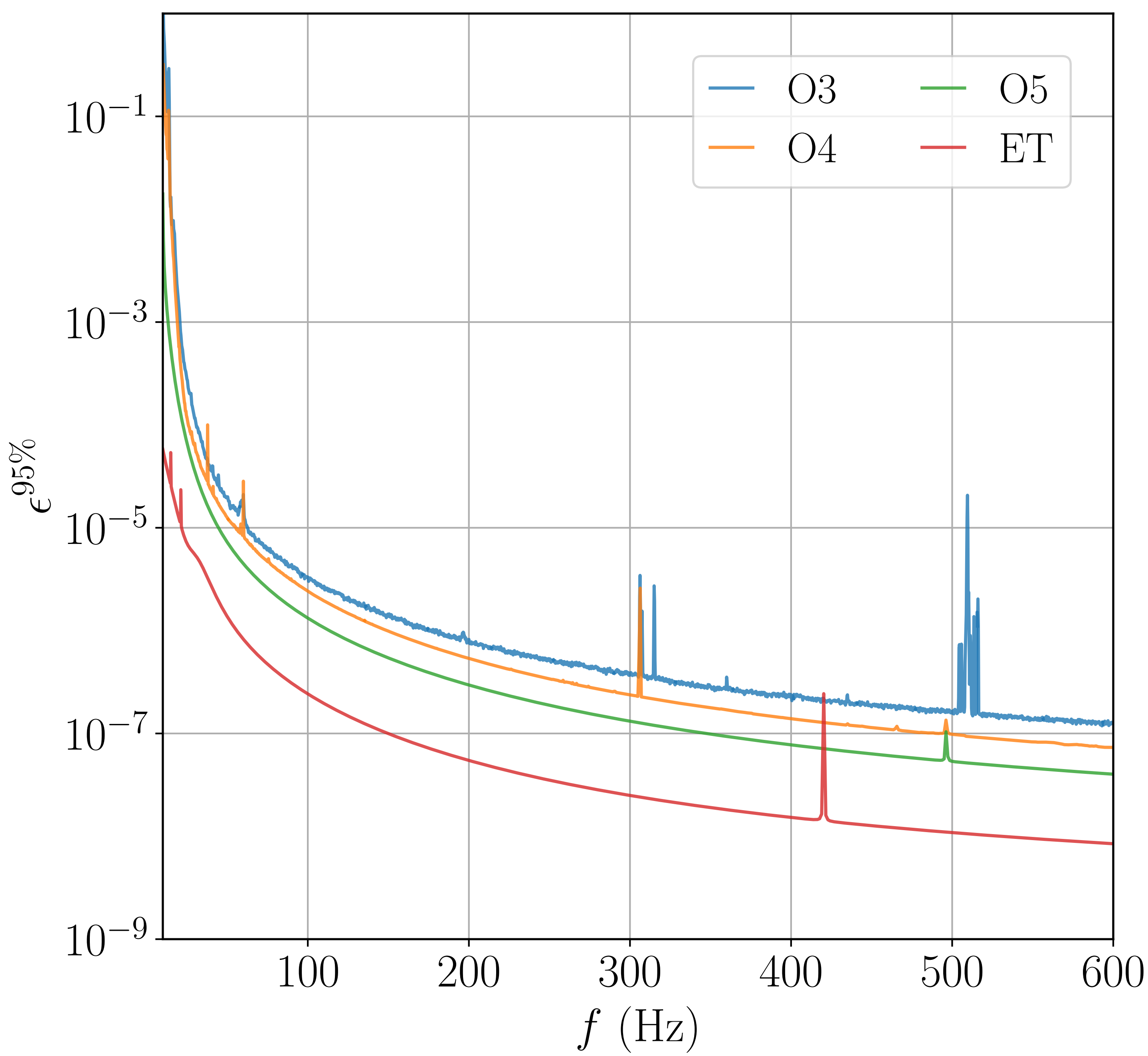

$$h_0 \propto \frac{I_3}{d}\epsilon f^2 \rightarrow \epsilon = \frac{c^4}{4\pi^2 G}\left(\frac{d}{I_3}\right)\frac{h_0}{f^2}$$

Vela Jr. distance d=1 kpc
$I_3 = I_{fid} = 10^{38}$ kg m^2

$10^{-9} \leq \epsilon \leq 10^{-4}$

from previous estimates

With a joint CW and EM observation we can measure NS radius, mass, magnetic field and ellipticity (EOS inference)

SOURCES FROM ASTRONOMICAL CATALOGS (O4+)

Sources which are likely hosting a NS are interesting candidates for CW searches.

The Fermi-LAT point sources catalog (4FGL):

identified (>30) or associated (>100) supernova remnants, pulsar wind nebula or globular clusters

unassociated sources (>1000)

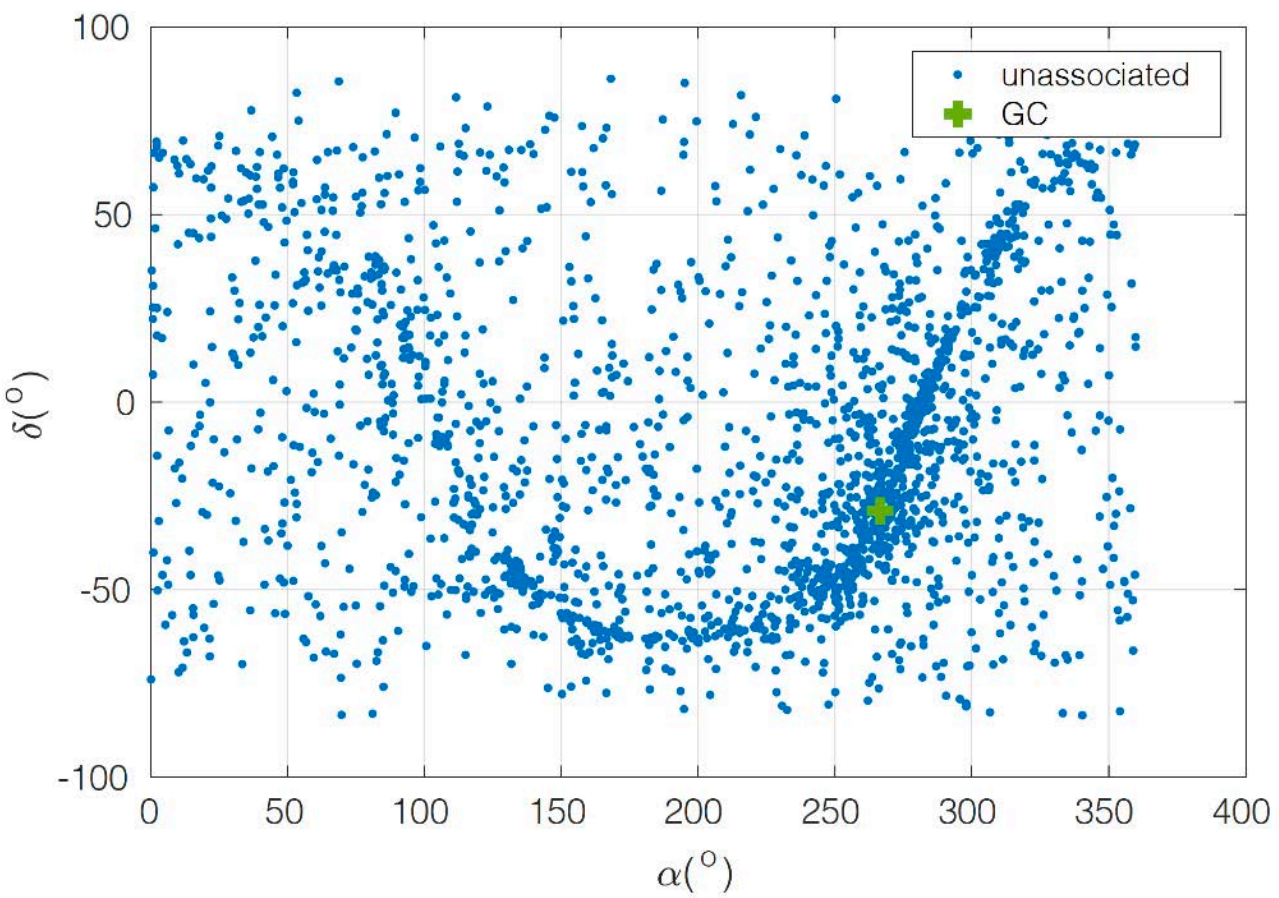

https://fermi.gsfc.nasa.gov/ssc/data/access/lat/8yr_catalog/

Unassociated: 1336 in Fermi-LAT we have only gamma-rays observation, no counterparts at other wavelengths

Estimates of the age and distance can be used to compute the *age based upper limit* h_{age}

optimal targets have h_{age} > pipeline sensitivity

SOURCES FROM ASTRONOMICAL CATALOGS (O4+)

the IBIS-INTEGRAL soft gamma-ray source catalog (Bird+ 2016):

- 10 SNR,
- 19 pulsar-like sources
- 216 unidentified ones (23%):

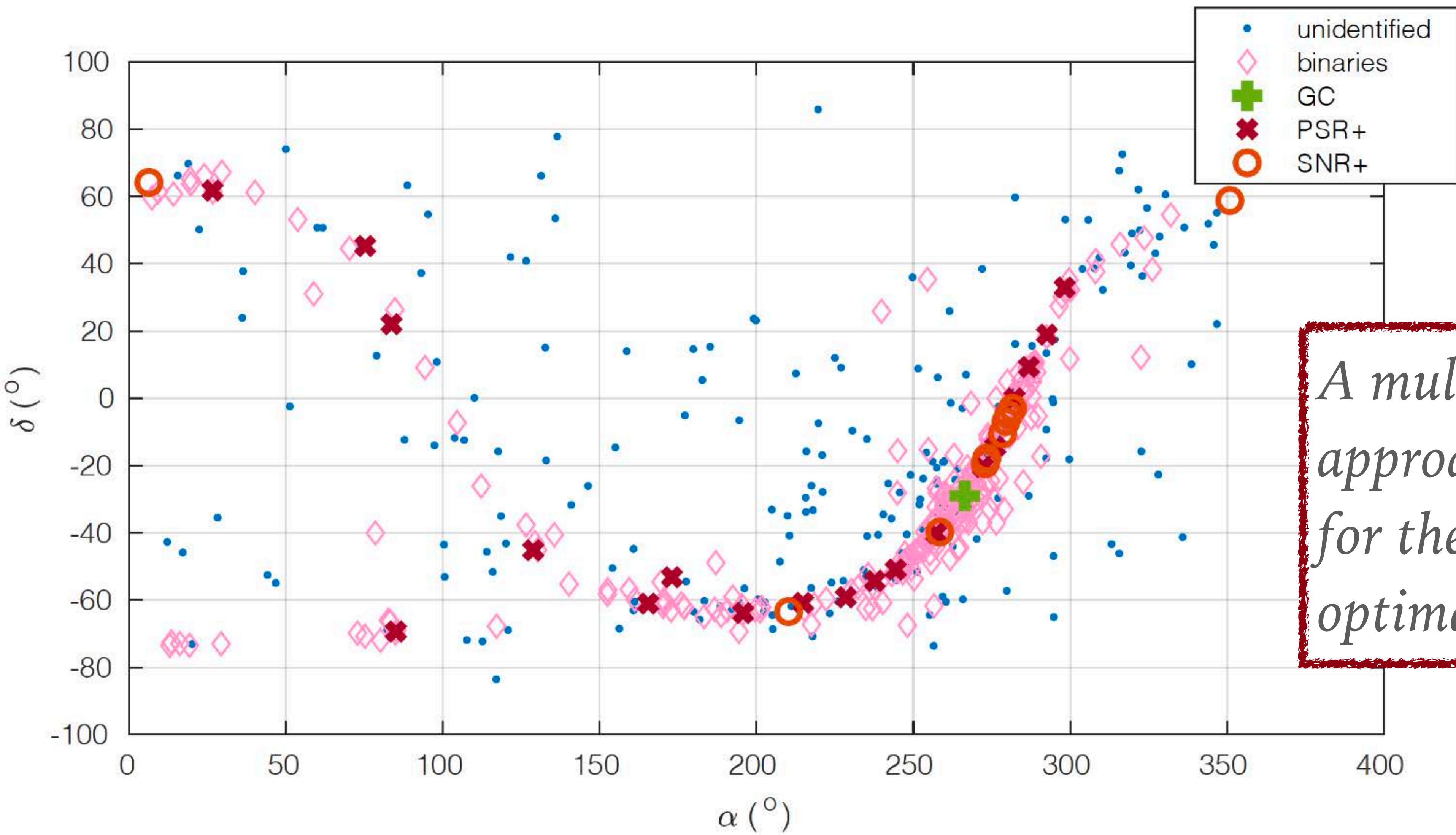

A multi-messenger approach is fundamental for the selection of optimal targets!

CONCLUSION

- CW could be the next surprise in GW astronomy given the enhanced sensitivity of the detectors, noise characterization is fundamental
- Efforts ongoing to increase the sensitivity of the pipelines
- For the standard NS case scenario we are probing ellipticities very close to the lowest estimates
- Exciting times especially if a joint CW and EM observation occurs (constraints on NS interior), remarking the importance of MMA.
- Searches for CWs emitted by standard and dual harmonic emission models are ongoing in O3 data, stay tuned
- We expect (and hope) to find several surprises in O4

This material is based upon work supported by NSF's LIGO Laboratory which is a major facility fully funded by the National Science Foundation. The authors also gratefully acknowledge the support of the Science and Technology Facilities Council (STFC) of the United Kingdom, the Max-Planck-Society (MPS), and the State of Niedersachsen/Germany for support of the construction of Advanced LIGO and construction and operation of the GEO600 detector. Additional support for Advanced LIGO was provided by the Australian Research Council. The authors gratefully acknowledge the Italian Istituto Nazionale di Fisica Nucleare (INFN), the French Centre National de la Recherche Scientifique (CNRS) and the Netherlands Organization for Scientific Research (NWO), for the construction and operation of the Virgo detector and the creation and support of the EGO consortium. The authors also gratefully acknowledge research support from these agencies as well as by the Council of Scientific and Industrial Research of India, the Department of Science and Technology, India, the Science & Engineering Research Board (SERB), India, the Ministry of Human Resource Development, India, the Spanish Agencia Estatal de Investigación, the Vicepresidència i Conselleria d'Innovació, Recerca i Turisme and the Conselleria d'Educació i Universitat del Govern de les Illes Balears, the Conselleria d'Innovació, Universitats, Ciència i Societat Digital de la Generalitat Valenciana and the CERCA Programme Generalitat de Catalunya, Spain, the National Science Centre of Poland and the European Union – European Regional Development Fund; Foundation for Polish Science (FNP), the Swiss National Science Foundation (SNSF), the Russian Foundation for Basic Research, the Russian Science Foundation, the European Commission, the European Regional Development Funds (ERDF), the Royal Society, the Scottish Funding Council, the Scottish Universities Physics Alliance, the Hungarian Scientific Research Fund (OTKA), the French Lyon Institute of Origins (LIO), the Belgian Fonds de la Recherche Scientifique (FRS-FNRS), Actions de Recherche Concertées (ARC) and Fonds Wetenschappelijk Onderzoek – Vlaanderen (FWO), Belgium, the Paris Ile-de-France Region, the National Research, Development and Innovation Office Hungary (NKFIH), the National Research Foundation of Korea, the Natural Science and Engineering Research Council Canada, Canadian Foundation for Innovation (CFI), the Brazilian Ministry of Science, Technology, and Innovations, the International Center for Theoretical Physics South American Institute for Fundamental Research (ICTP-SAIFR), the Research Grants Council of Hong Kong, the National Natural Science Foundation of China (NSFC), the Leverhulme Trust, the Research Corporation, the Ministry of Science and Technology (MOST), Taiwan, the United States Department of Energy, and the Kavli Foundation. The authors gratefully acknowledge the support of the NSF, STFC, INFN and CNRS for provision of computational resources.

This work was supported by MEXT, JSPS Leading-edge Research Infrastructure Program, JSPS Grant-in-Aid for Specially Promoted Research 26000005(Kajita 2014-2018), JSPS Grant-in-Aid for Scientific Research on Innovative Areas 2905: JP17H06358, JP17H06361 and JP17H06364, JSPS Core-to-Core Program A. Advanced Research Networks, JSPS Grant-in-Aid for Scientific Research (S) 17H06133 and 20H05639, JSPS Grant-in-Aid for Transformative Research Areas (A) 20A203: JP20H05854, the joint research program of the Institute for Cosmic Ray Research, University of Tokyo, National Research Foundation (NRF) and Computing Infrastructure Project of KISTI-GSDC in Korea, Academia Sinica (AS), AS Grid Center (ASGC) and the Ministry of Science and Technology (MoST) in Taiwan under grants including AS-CDA-105-M06, Advanced Technology Center (ATC) of NAOJ, Mechanical Engineering Center of KEK.